

First-principles prediction of phonon-mediated superconductivity in XBC ($X = \text{Mg, Ca, Sr, Ba}$)

Enamul Haque and M. Anwar Hossain*
Department of Physics,
Mawlana Bhashani Science and Technology University
Santosh, Tangail-1902, Bangladesh

Catherine Stampfl†
School of Physics, The University of Sydney, Sydney,
New South Wales, 2006, Australia.
 (Dated: July 27, 2021)

From first-principles calculations, we predict four new intercalated hexagonal XBC ($X = \text{Mg, Ca, Sr, Ba}$) compounds to be dynamically stable and phonon-mediated superconductors. These compounds form a LiBC like structure but are metallic. The calculated superconducting critical temperature, T_c , of MgBC is 51 K. The strong attractive interaction between σ -bonding electrons and the B_{1g} phonon mode gives rise to a larger electron-phonon coupling constant (1.135) and hence high T_c ; notably, higher than that of MgB_2 . The other compounds have a low superconducting critical temperature (4-17 K) due to the interaction between σ -bonding electrons and low energy phonons (E_{2u} modes). Due to their energetic and dynamic stability, we envisage that these compounds can be synthesized experimentally.

PACS numbers: 63.20.dk, 74.25.Kc, 63.20.kd, 74.20.Pq, 74.70.-b

Hexagonal layered MgB_2 is a well-known phonon-mediated superconductor with a $T_c = 39$ K [1]. In MgB_2 , the σ -band crosses the Fermi level and hybridization with other conduction electrons is weak. The high T_c -state of this material develops from the strong attractive interaction between the electrons of the σ -band and the E_{2g} mode of vibrations. Likely MgB_2 , materials intercalated with alkali (earth) metals show superconductivity with T_c much smaller than that of MgB_2 [2–13]. Many studies have proposed possible ways to improve the transition temperature through carbon (or others) doping [14–16]. However, the T_c has not been found to improve significantly [14–19]. The T_c decreases on carbon substitution of B in MgB_2 due to the introduction simultaneous disorder by carbon [16, 18, 20, 21]. Thus, it may be an alternative to examine the superconducting properties by synthesizing pure MgBC compounds.

From the first-principles investigations of LiBC with hole-doping, it was found to exhibit superconductivity below 100 K [22]. Unfortunately, experimentalists have not identified superconductivity in it due to induced structural distortions [23–27]. This is a similar effect to that of carbon doping in MgB_2 . Recently, $\text{LiB}_{1+x}\text{C}_{1-x}$ materials have been predicted to be superconductors, like MgB_2 [28]. Also on the basis of first-principles calculations, Gao *et al.* reported $\text{Li}_3\text{B}_4\text{C}_2$ (also $\text{Li}_2\text{B}_3\text{C}$) to be MgB_2 like superconductor with $T_c \sim 53$ K [27]. Since then, another phase, $\text{Li}_4\text{B}_5\text{C}_3$, has been reported from ab initio studies to be a superconductor with a transition temperature of 16.8 K [29]. From the first-principles study of $\text{NaB}_{1+x}\text{C}_{1-x}$, Miao *et al.* predicted

that it would be more promising superconductor than $\text{LiB}_{1-x}\text{C}_x$ [30]. Like LiBC, Ravindran *et al.* predicted that hole-doped MgB_2C_2 is a potential superconducting material [31]. Since high-quality single crystals of LiBC have already been synthesized [16,17], it may be possible to synthesize XBC ($X = \text{Mg, Ca, Sr, Ba}$). In the present paper, we report, using the first-principles calculations, four new superconducting stoichiometric compounds (XBC ($X = \text{Mg, Ca, Sr, Ba}$)) that are dynamically stable and may be synthesized from constituent elemental solids. We find that strong electron-phonon interactions exist in all these materials. The MgBC structure has a predicted T_c (~ 51 K) higher than that of MgB_2 ; while SrBC and BaBC have a superconducting state below ~ 17 K (The CaBC structure has very small T_c (4 K)).

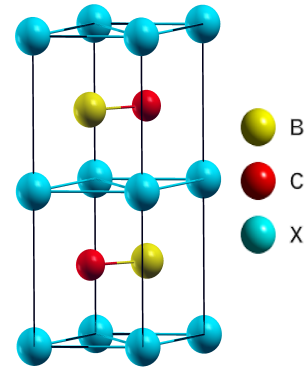


FIG. 1. The ground state crystal structure of XBC ($X = \text{Mg, Ca, Sr, Ba}$). The X, B, and C atoms are indicated by cyan, yellow, and red spheres, respectively.

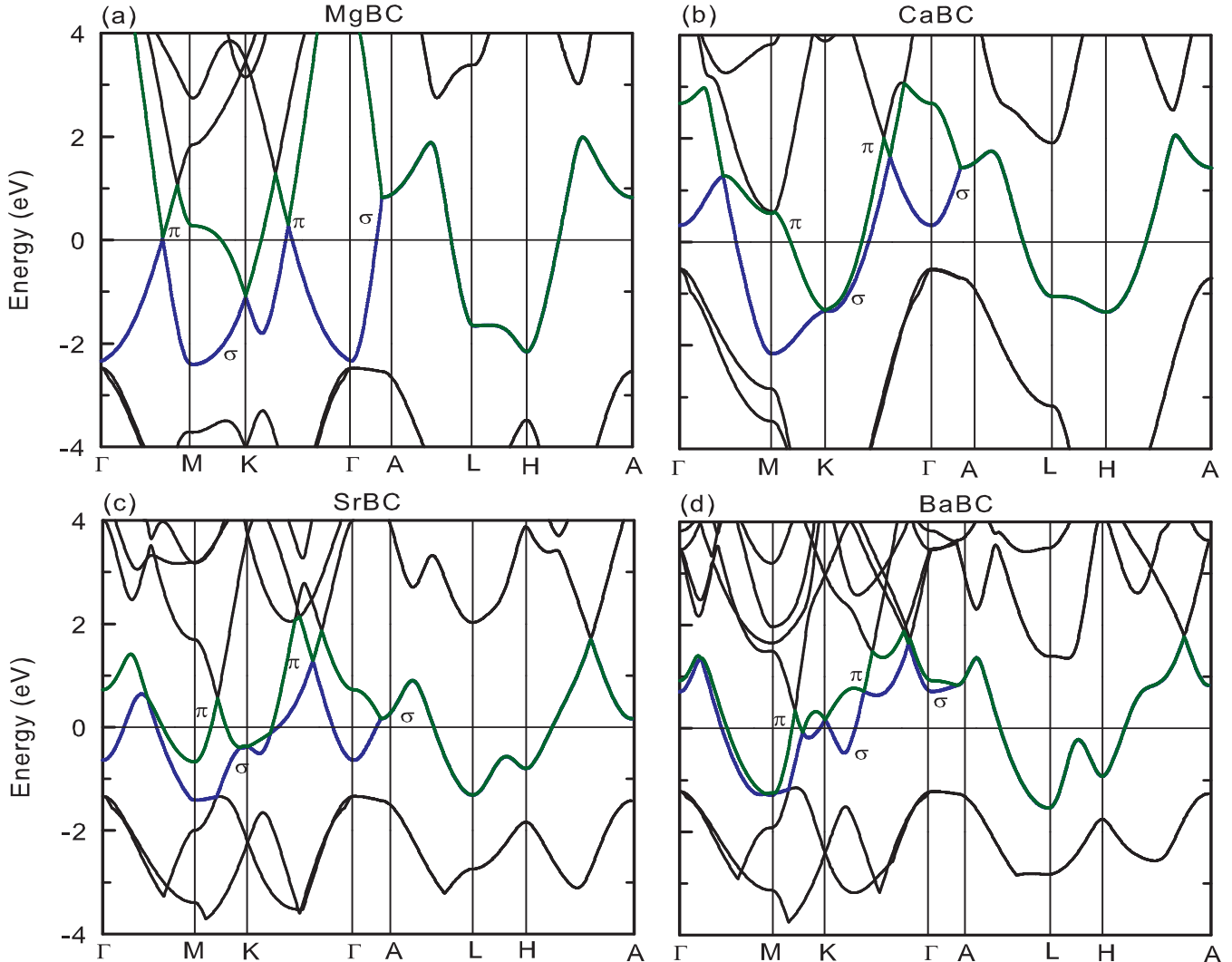


FIG. 2. Electronic band structure of the four compounds: (a) MgBC, (b) CaBC, (c) SrBC, and (d) BaBC. The Fermi level is the zero of energy. The blue and red curves with symbols represent the energy bands that cross the Fermi level and form the Fermi surface. We have selected high-symmetry \mathbf{k} -points in the Brillouin zone and the values of them in fractional coordinates are $\Gamma(0,0,0)$, $M(1/2,0,0)$, $K(1/3,1/3,0)$, $A(0,0,1/2)$, $L(1/2,0,1/2)$, and $H(1/3,1/3,1/2)$.

All calculations were performed using the plane wave pseudopotential approach and the generalized gradient approximation of Perdew-Burke-Ernzerhof (PBE-GGA) [32, 33] for the exchange correlation functional, as implemented in Quantum Espresso [34]. We use the ultrasoft pseudopotentials of Vanderbilt [35] and perform full structural relaxation. After optimizing the \mathbf{k} -point mesh and cutoff energy, we selected a $12 \times 12 \times 4$ \mathbf{k} -point mesh for self-consistent field calculations, a 50 Ry cutoff energy for the wave functions, and a 400 Ry energy cutoff for the charge density. For the phonon calculations, we use a 662 grid of uniform \mathbf{q} -points and the same \mathbf{k} -point mesh as above [36]. We used a

finer $18 \times 18 \times 6$ \mathbf{k} -point mesh for the calculation of the electron-phonon (e-ph) linewidth and e-ph coupling constants employing the optimized tetrahedron method in e-ph calculation [37]. We performed the phonon calculations using density functional perturbation theory (DFPT) of linear response [38]. For the electron-phonon coupling constant (EPC) calculations, we used the Migdal-Eliashberg formalism [39]. In this formalism, the Eliashberg spectral function is defined as [40, 41]

$$\alpha^2 F(\omega) = \frac{1}{2\pi N(E_F)} \sum_{\mathbf{qv}} \delta(\omega - \omega_{\mathbf{qv}}) \frac{\gamma_{\mathbf{qv}}}{\hbar\omega_{\mathbf{qv}}} \quad (1)$$

where $N(E_F)$ is the density of states at the Fermi level

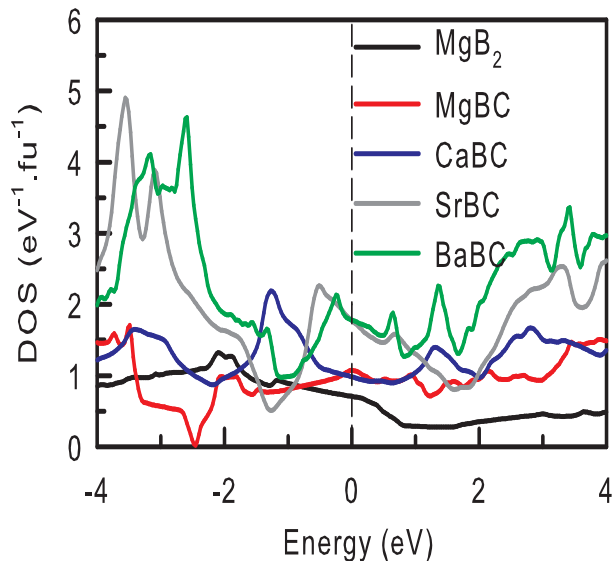


FIG. 3. Calculated total density of states (DOS) of XBC ($X=\text{Mg, Ca, Sr, Ba}$) within the energy range from -4 to 4 . The Fermi level is the zero of energy and indicated by the vertical dashed line.

and $\gamma_{q\mathbf{v}}$ is the electron-phonon linewidth for wave vectors \mathbf{q} and \mathbf{v} . The EPC is determined by [40, 41]

$$= 2 \int \frac{\alpha^2 F(\omega)}{\omega} d\omega. \quad (2)$$

Using the calculated EPC, the superconducting transition temperature is evaluated by the Allen-Dynes equation [40, 41]

$$T_c = \frac{\omega_{ln}}{1.2} \exp \left[\frac{(-1.04(1 + \lambda))}{(\lambda(1 - 0.62\mu^*) - \mu^*)} \right] \quad (3)$$

where μ^* stands for the Coulomb pseudopotential constant and its value ranges between 0.1 and 0.15 [42, 43]. ω_{ln} stands for the logarithmic average frequency and is defined as [40, 41]

$$\omega_{ln} = \exp \left[\frac{2}{\lambda} \int \frac{d\omega}{\omega} \alpha^2 F(\omega) \ln(\omega) \right]. \quad (4)$$

The crystal structure of XBC ($X=\text{Mg, Ca, Sr, Ba}$) is similar to that of MgB_2 . X atoms have no bonds with either B or C. Boron and carbon are bonded together in a primitive fashion. Unlike MgB_2 , the unit cell contains six equivalent atoms, two of each species. Figure 1 shows the hexagonal crystal structure of XBC ($X=\text{Mg, Ca, Sr, Ba}$). Our theoretical value of the lattice parameters of MgB_2 is in a good agreement with the experimental value ($a = 3.086\text{\AA}$ and $c/a = 1.42$) [1], as listed in table 1.

TABLE I. Calculated fully relaxed lattice parameters of MgB_2 and XBC of ($X=\text{Mg, Ca, Sr, Ba}$).

Compounds	$a(\text{\AA})$	c/a
MgB_2	3.081	1.145
MgBC	2.808	2.608
CaBC	2.951	2.745
SrBC	3.013	2.973
BaBC	3.084	3.190

The fully relaxed lattice constant along the a -axis is close to the value of MgB_2 while that along the c -axis of all compounds become around twice that of MgB_2 (see Table 1). We have found that all the studied compounds are energetically stable [44]. The electronic band structures of the four compounds are shown in figure 2. All the compounds possess metallic character. We see that two energy bands cross the Fermi level and form the Fermi surface for all materials. The symbols, σ and π , indicate the type of bonding electrons belonging to the energy bands crossing the Fermi level. These bands are highly dispersive along all directions except L-H. These bands are slightly flat along A-L above E_F and L-H below E_F . The bands crossing the Fermi level are doubly degenerate along the Γ -A direction.

If we compare the band structure of MgBC and CaBC , we see that the Fermi level in CaBC is shifted to higher energy than that of MgBC . Therefore, this may lead to a reduction of T_c or eliminate the superconducting state of CaBC . However, the shift in energy of SrBC and BaBC is small as compared to CaBC .

Figure 3 shows the calculated total density of states of XBC ($X=\text{Mg, Ca, Sr, Ba}$). The density of states at the Fermi level has increased significantly in all the studied compounds compared to MgB_2 . In the case of CaBC , the DOS at the Fermi level is similar to MgBC and notably lower than both of SrBC and BaBC . As mentioned above, the DOS of MgBC at the Fermi level is much increased in comparison with that of MgB_2 for the electron injected by carbon [45]. Since the σ -band crosses the Fermi level, σ -bonding electrons can strongly attract certain modes of vibration, like the E_{2g} mode of MgB_2 . Therefore, all compounds should be superconductors at a certain temperature. We will now investigate the electron-phonon coupling within Migdal-Eliashberg formalism.

The dynamical stability of a crystal is an important criterion in order to be able to synthesize it. Many researchers have reported the failure of synthesis of potentially promising materials due to dynamical instability [46]. The phonons determine the dynamical stability of a crystal; if any imaginary frequencies appears in the phonon band structure, the crystal structure is dynamically unstable. Recently, Kato *et al.*

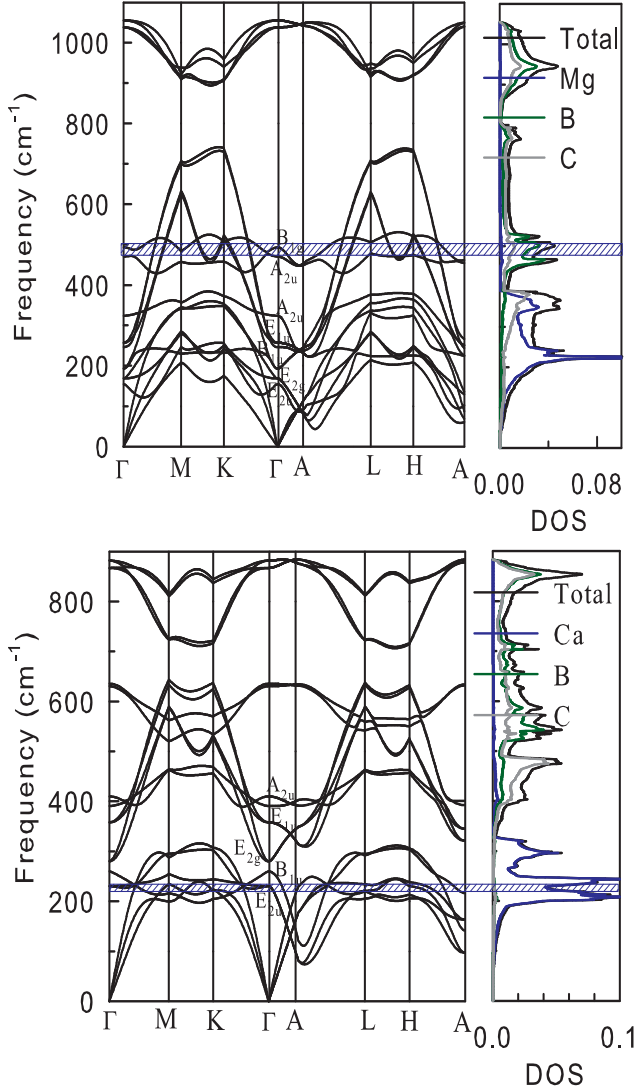


FIG. 4. Phonon dispersion relations, total, and atom projected phonon density of states of MgBC (top panel) and CaBC (bottom panel). The blue shaded area indicates the modes of the region where electrons are strongly coupled.

reported the possibility of MgB₂-like superconductivity in MgBY (Y=C, Be, Li) from electronic band structure analysis without considering the dynamical stability of these compounds [47]. They also predicted that MgBC might not be a two-band superconductor because the σ -band is completely filled. We note that the lattice constant of dynamically stable MgBC along the c -axis is twice as large as that of considered the one in their study [47], i.e., it has different atomic structure. The Fermi level in MgBC is raised to higher energy, even around the sigma anti-bonding states, compared to that of MgB₂. In this respect, MgBC is different in electronic structure to that of MgB₂.

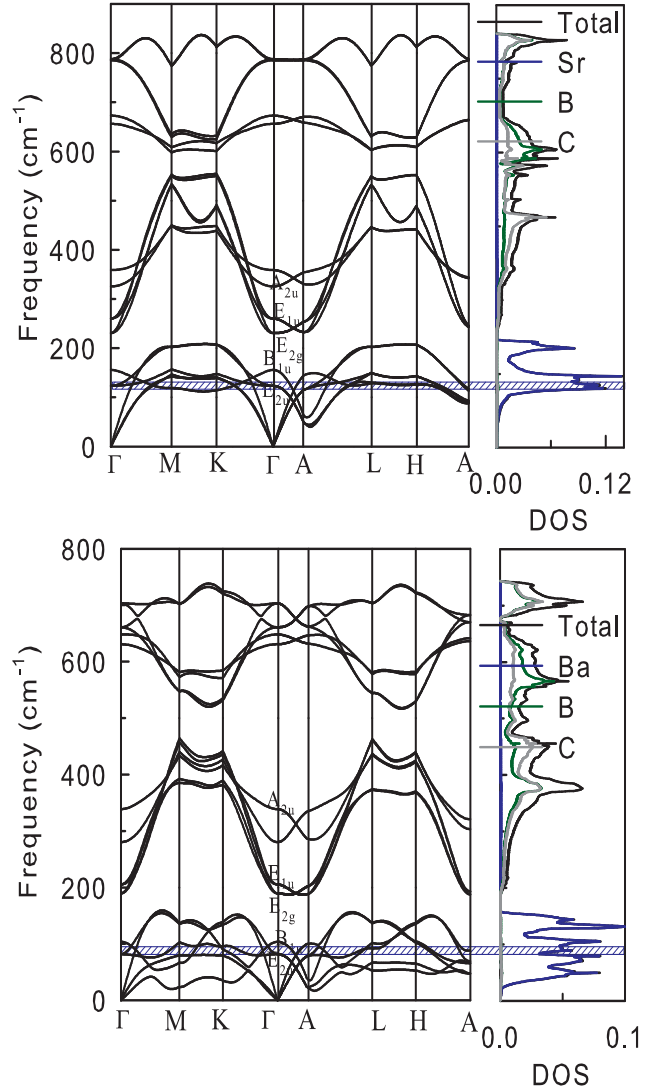


FIG. 5. Phonon band structures, total, and atom projected phonon density of states of SrBC (top panel) and BaBC (bottom panel). The blue shaded area indicates the modes of the region (E_{2u}) where electrons are strongly coupled.

Figure 4 shows the phonon dispersion relation and phonon density of states (DOS) of MgBC (upper panel) and CaBC (lower panel). We see that no imaginary frequency appears in the phonon band structure for both compounds. Therefore, hexagonal MgBC and CaBC are dynamically stable [48]. Low energy phonons mainly arise from Mg and Ca in MgBC, and CaBC respectively. Higher energy phonons arise from B and C in both compounds. In MgBC, the optical Γ -center modes are shifted to higher frequencies as compared to MgB₂. In contrast to MgB₂ (where the in-plane boron mode is E_{2g}), the B-C in-plane phonon at the

Γ -point is the B_{1g} mode where electrons are strongly coupled, as indicated by the shaded area in figure 4. The shaded area corresponds to the highest peak region in the Eliashberg spectral function. The corresponding frequency of the B_{1g} mode at the Γ -point is 495 cm^{-1} , which is much smaller than that of the value of 692 cm^{-1} for MgB_2 [49].

For CaBC, low energy phonons of the E_{2u} mode region arise from Ca atom and in this region, electrons are strongly coupled (maximum peak region in the Eliashberg spectral function). Higher energy phonons arising from B and C have very small contributions to electron-phonon interactions. Since the density of states (DOS) at the Fermi level of CaBC (see figure 3) is reduced as compared to MgBC, and the phonon frequency too (blue shaded region), σ -band electrons are not so strongly coupled with E_{2u} modes of the phonons as like in MgB_2 . Therefore, CaBC cannot be a MgB_2 -like superconductor.

The phonon energy of the blue shaded area at Γ -point is more reduced in SrBC and BaBC compared to CaBC, as shown in figure 5. Like CaBC, SrBC, and BaBC have E_{2u} modes region where electrons are strongly coupled. However, unlike CaBC, the density of states of SrBC and BaBC at the Fermi level are notably higher. Therefore, electrons should be more strongly coupled than those in CaBC. For hexagonal SrBC and BaBC, we do not obtain any imaginary frequencies. Therefore, both structures are energetically [44] and dynamically stable [48]. The phonon density of states of MgBC exhibits three distinct peaks; in contrast MgB_2 has only one peak [18]. The first peak arises from the Mg of E_{1u} mode and the second and third peaks arise from B and C. The second peak shows that B has a dominant contribution. The Eliashberg spectral function of MgBC also shows three peaks, in comparison with just one peak of MgB_2 . The main peak around 694 cm^{-1} arises from the predominant interaction between σ -band electrons and the B_{1g} phonon mode. These three peaks in the Eliashberg spectral function are shifted to lower energy phonons (E_{2u}) in the case of the other remaining three compounds. For CaBC, the highest peak height is almost half of the highest peak height for MgBC, SrBC, and BaBC. From the Eliashberg spectral function, we can calculate the electron-phonon coupling constant, logarithmic average phonon frequency and hence the superconducting transition temperature using the Allen-Dynes equation [41]. Our calculated superconducting parameters of the four compounds are listed in Table 2. In the table, we have used the value of the Coulomb pseudopotential to be 0.1.

For MgB_2 , our calculated electron-phonon coupling constant (λ) is 0.844, in a good agreement with the available results [27, 49] but slightly smaller than that of the value reported in Ref. [50]. This value is slightly larger than that of the obtained value by using Wannier in-

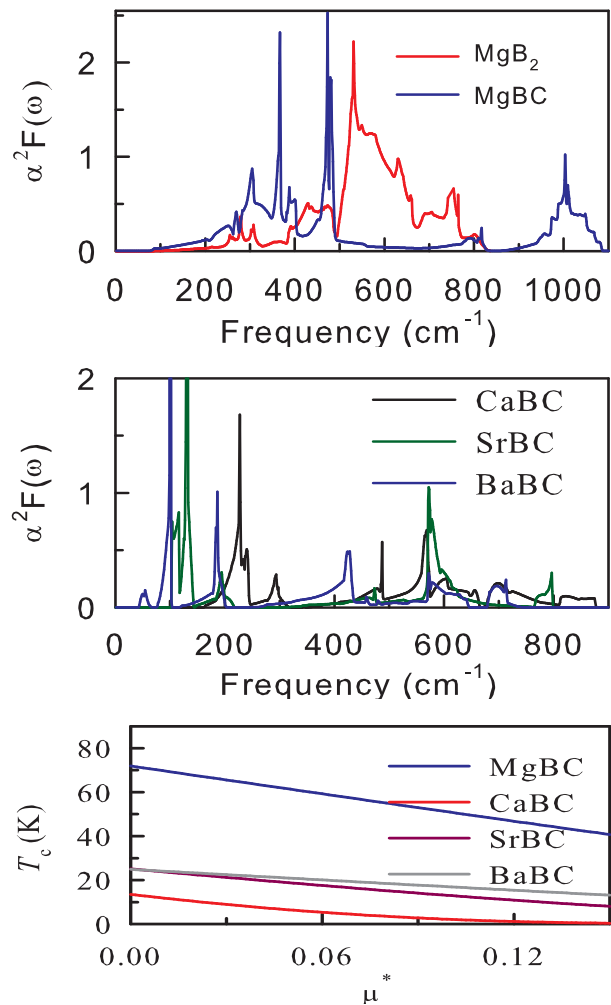


FIG. 6. Calculated Eliashberg spectral function $\alpha^2 F(\omega)$ of MgB_2 and MgBC (upper panel), and of CaBC, SrBC, BaBC (middle panel). The lower panel shows calculated superconducting transition temperature as a function of μ^* .

TABLE II. Calculated superconducting parameters of fully relaxed structures XBC of ($X=\text{Mg}, \text{Ca}, \text{Sr}, \text{Ba}$). We have used the value of μ^* to be 0.1 in Eqn. (3).

Compounds	$\omega_{ln}(\text{K})$	λ	$T_c(\text{K})$
MgBC	610.05	1.135	51
CaBC	723.09	0.377	4
SrBC	382.27	0.693	13
BaBC	231.13	1.034	17

terpolation method [51–53]. We find that the logarithmic average phonon frequency (ω_{ln}) is 708 K, in a good agreement with available data [27, 49, 54–58]. We obtain $T_c = 37\text{K}$ by using $\mu^* = 0.1$, slightly smaller than that of the experimental value (39 K). We see that the maximum superconducting transition temperature is obtained for MgBC and minimum for CaBC. The electron-phonon coupling constant (1.135) of MgBC is a 26% larger than

that obtained for MgB₂ (0.87-0.88) [27, 49, 50]. Thus, if we use the value of μ^* to be 0, we obtain $T_c=72$ K for MgBC. Even if we use the value of 0.15 for μ^* , we still obtain a superconducting transition temperature above 40 K. Therefore, MgBC is a phonon-mediated superconductor with larger electron-phonon coupling constant and higher transition temperature than MgB₂. The larger electron-phonon coupling constant of MgBC arises from three peaks in the phonon density of states, mainly due to the strong coupling of σ -band electrons with the B_{1g} phonon mode. The others three compounds have a lower transition temperature compared to MgB₂.

In summary, we have predicted four new superconductors using the first-principles calculations. Hexagonal XBC ($X=\text{Mg, Ca, Sr, Ba}$) compounds are found to be phonon-mediated superconductors. Among these compounds, the calculated T_c of MgBC is 51 K. The strong coupling between σ -bonding electrons and the B_{1g} phonon mode gives rise to a larger electron-phonon coupling and hence high T_c . Thus, MgBC is a superconductor with T_c higher than that of MgB₂. The other compounds have a low superconducting transition temperature due to the interaction between σ -bonding electrons and low energy phonons (E_{2u} modes).

We must thank W.E Pickett for giving some helpful suggestions and critical reading of the manuscript.

* anwar647@mbstu.ac.bd, enamul.phy15@yahoo.com

† catherine.stampfl@sydney.edu.au

- [1] J. Nagamatsu, N. Nakagawa, T. Muranaka, Y. Zenitani, and J. Akimitsu, *nature* **410**, 63 (2001).
- [2] N. Hannay, T. Geballe, B. Matthias, K. Andres, P. Schmidt, and D. MacNair, *Physical Review Letters* **14**, 225 (1965).
- [3] I. Belash, A. Bronnikov, O. Zharikov, and A. Pal'nichenko, *Solid State Communications* **69**, 921 (1989).
- [4] N. Emery, C. Hérold, M. dAstuto, V. Garcia, C. Bellin, J. Maréché, P. Lagrange, and G. Louprias, *Physical Review Letters* **95**, 087003 (2005).
- [5] M. Calandra and F. Mauri, *Physical Review Letters* **95**, 237002 (2005).
- [6] G. Csányi, P. Littlewood, A. H. Nevidomskyy, C. J. Pickard, and B. Simons, *Nature Physics* **1**, 42 (2005).
- [7] G. Profeta, M. Calandra, and F. Mauri, *Nature Physics* **8**, 131 (2012).
- [8] A. Sanna, G. Profeta, A. Floris, A. Marini, E. Gross, and S. Massidda, *Physical Review B* **75**, 020511 (2007).
- [9] A. Gauzzi, S. Takashima, N. Takeshita, C. Terakura, H. Takagi, N. Emery, C. Hérold, P. Lagrange, and G. Louprias, *Physical Review Letters* **98**, 067002 (2007).
- [10] A. P. Tiwari, S. Shin, E. Hwang, S.-G. Jung, T. Park, and H. Lee, *Journal of Physics: Condensed Matter* **29**, 445701 (2017).
- [11] S. Nishiyama, H. Fujita, M. Hoshi, X. Miao, T. Terao, X. Yang, T. Miyazaki, H. Goto, T. Kagayama, K. Shimizu, *et al.*, *Scientific Reports* **7**, 7436 (2017).
- [12] J.-H. Liao, Y.-C. Zhao, Y.-J. Zhao, H. Xu, and X.-B. Yang, *Physical Chemistry Chemical Physics* **19**, 29237 (2017).
- [13] S. A. Tawfik, C. Stampfl, and M. J. Ford, *Physical Chemistry Chemical Physics* **20**, 24027 (2018).
- [14] A. Bharathi, Y. Hariharan, J. Balaselvi, and C. Sundar, *Sadhana* **28**, 263 (2003).
- [15] B. Jemima, A. Bharathi, S. Sankara, G. Reddy, Y. Hariharan, *et al.*, in *Proceedings of the DAE solid state physics symposium. V. 45* (2003).
- [16] S. Kazakov, R. Puzniak, K. Rogacki, A. Mironov, N. Zhigadlo, J. Jun, C. Soltmann, B. Batlogg, and J. Karpinski, *Physical Review B* **71**, 024533 (2005).
- [17] S. J. Balaselvi, N. Gayathri, A. Bharathi, V. Sastry, and Y. Hariharan, *Superconductor Science and Technology* **17**, 1401 (2004).
- [18] E. Ohmichi, T. Masui, S. Lee, S. Tajima, and T. Osada, *Journal of the Physical Society of Japan* **73**, 2065 (2004).
- [19] A. Bharathi, S. J. Balaselvi, S. Kalavathi, G. Reddy, V. S. Sastry, Y. Hariharan, and T. Radhakrishnan, *Physica C: Superconductivity* **370**, 211 (2002).
- [20] V. Braccini, A. Gurevich, J. Giencke, M. Jewell, C. Eom, D. Larbalestier, A. Pogrebnnyak, Y. Cui, B. Liu, Y. Hu, *et al.*, *Physical Review B* **71**, 012504 (2005).
- [21] M. Pissas, D. Stamopoulos, S. Lee, and S. Tajima, *Physical Review B* **70**, 134503 (2004).
- [22] H. Rosner, A. Kitaigorodsky, and W. Pickett, *Physical Review Letters* **88**, 127001 (2002).
- [23] A. Fogg, P. Chalker, J. Claridge, G. Darling, and M. Rosseinsky, *Physical Review B* **67**, 245106 (2003).
- [24] A. M. Fogg, J. Meldrum, G. R. Darling, J. B. Claridge, and M. J. Rosseinsky, *Journal of the American Chemical Society* **128**, 10043 (2006).
- [25] D. Souptel, Z. Hossain, G. Behr, W. Löser, and C. Geibel, *Solid State Communications* **125**, 17 (2003).
- [26] A. Bharathi, S. J. Balaselvi, M. Premila, T. Sairam, G. Reddy, C. Sundar, and Y. Hariharan, *Solid State Communications* **124**, 423 (2002).
- [27] M. Gao, Z.-Y. Lu, and T. Xiang, *Physical Review B* **91**, 045132 (2015).
- [28] Q.-Z. Li, X.-W. Yan, M. Gao, and J. Wang, *Europhysics Letters* **122**, 47001 (2018).
- [29] T. Bazhurov, Y. Sakai, S. Saito, and M. L. Cohen, *Physical Review B* **89**, 045136 (2014).
- [30] R. Miao, G. Huang, and J. Yang, *Solid State Communications* **233**, 30 (2016).
- [31] P. Ravindran, P. Vajeeston, R. Vidya, A. Kjekshus, and H. Fjellvåg, *Physical Review B* **64**, 224509 (2001).
- [32] J. P. Perdew, K. Burke, and M. Ernzerhof, *Physical Review Letters* **77**, 3865 (1996).
- [33] J. P. Perdew, A. Ruzsinszky, G. I. Csonka, O. A. Vydrov, G. E. Scuseria, L. A. Constantin, X. Zhou, and K. Burke, *Physical Review Letters* **100**, 136406 (2008).
- [34] P. Giannozzi, S. Baroni, N. Bonini, M. Calandra, R. Car, C. Cavazzoni, D. Ceresoli, G. L. Chiarotti, M. Cococcioni, I. Dabo, *et al.*, *Journal of Physics: Condensed Matter* **21**, 395502 (2009).
- [35] D. Vanderbilt, *Physical Review B* **41**, 7892 (1990).
- [36] We use same the cutoff energy and a 666 uniform grid of \mathbf{q} -point for MgB₂. For calculation of the electron-phonon coupling constant and Fermi surface evaluation, we use a $24 \times 24 \times 24$ \mathbf{k} -point mesh.
- [37] M. Kawamura, Y. Gohda, and S. Tsuneyuki, *Physical Review B* **89**, 094515 (2014).

- [38] S. Baroni, S. De Gironcoli, A. Dal Corso, and P. Gianozzi, *Reviews of Modern Physics* **73**, 515 (2001).
- [39] G. Eliashberg, *Sov. Phys. JETP* **11**, 696 (1960).
- [40] P. B. Allen, *Physical Review B* **6**, 2577 (1972).
- [41] P. B. Allen and R. Dynes, *Physical Review B* **12**, 905 (1975).
- [42] C. Richardson and N. Ashcroft, *Physical Review Letters* **78**, 118 (1997).
- [43] K.-H. Lee, K.-J. Chang, and M. L. Cohen, *Physical Review B* **52**, 1425 (1995).
- [44] The formation energy is calculated by taking the energy difference between the total energy of the compound and sum of the energy of individual constituent elements in their stable structure. We used hexagonal-Mg, face-centered cubic Ca and Sr, body-centered cubic Ba, graphite (C), and α - B_{12} type structure of boron [60]. Our calculated formation energies of MgBC, CaBC, SrBC and BaBC are -0.14 , -0.13 , 0.73 and 1.5 eV.fu $^{-1}$, respectively. Although the formation energy of MgBC is small, the negative value of the formation energy of the first two compounds indicates a high possibility of synthesis of first two compounds in the laboratory. However, the positive formation energy of SrBC and BaBC indicates difficulty in the synthesis. The non-equilibrium methods of growth (epitaxial technique) may be used to synthesis these compounds (as a metastable structure), although it might be difficult.
- [45] I. Mazin and V. Antropov, *Physica C: Superconductivity* **385**, 49 (2003).
- [46] G. Grimvall, B. Magyari-Köpe, V. Ozoliņš, and K. A. Persson, *Reviews of Modern Physics* **84**, 945 (2012).
- [47] N. Kato, H. Nagao, K. Nishikawa, K. Nishidate, and K. Endo, *International Journal of Quantum Chemistry* **96**, 457 (2004).
- [48] The large value of electron-phonon coupling of MgBC may give rise to the question of the lattice instability. All the predicted compounds have 18 independent vibrational modes. We have calculated the frequencies of each mode by using a uniform $q_1 \times q_1 \times q_2$ grid, where q_1 has been varied from 4 to 8 and q_2 from 2 to 4. We do not find any imaginary frequencies at these phonon wave vectors and along the considered high-symmetry \mathbf{k} -points. Moreover, we have calculated the phonon dispersion using a Mazari Vanderbilt smearing of width 0.08 Ry and obtained the same phonon dispersion curves. Furthermore, we have calculated the phonon dispersion using the finite displacement method in the Phonopy program [59] and obtained identical results. The obtained phonon dispersion curves suggest that XBC are dynamically stable.
- [49] Y. Kong, O. Dolgov, O. Jepsen, and O. Andersen, *Physical Review B* **64**, 020501 (2001).
- [50] T. Yildirim, O. Gülseren, J. Lynn, C. Brown, T. Udovic, Q. Huang, N. Rogado, K. Regan, M. Hayward, J. Slusky, *et al.*, *Physical Review Letters* **87**, 037001 (2001).
- [51] A. Eiguren and C. Ambrosch-Draxl, *Physical Review B* **78**, 045124 (2008).
- [52] M. Calandra, G. Profeta, and F. Mauri, *Physical Review B* **82**, 165111 (2010).
- [53] E. R. Margine and F. Giustino, *Physical Review B* **87**, 024505 (2013).
- [54] J. An and W. Pickett, *Physical Review Letters* **86**, 4366 (2001).
- [55] H. J. Choi, D. Roundy, H. Sun, M. L. Cohen, and S. G. Louie, *Physical Review B* **66**, 020513 (2002).
- [56] H. J. Choi, D. Roundy, H. Sun, M. L. Cohen, and S. G. Louie, *Nature* **418**, 758 (2002).
- [57] K.-P. Bohnen, R. Heid, and B. Renker, *Physical Review Letters* **86**, 5771 (2001).
- [58] T. Morshedloo, M. Roknabadi, and M. Behdani, *Physica C: Superconductivity and its Applications* **509**, 1 (2015).
- [59] A. Togo and I. Tanaka, *Scripta Materialia* **108**, 1 (2015).
- [60] B. Decker and J. Kasper, *Acta Crystallographica* **12**, 503 (1959).